JOURNAL OF THERMOPHYSICS AND HEAT TRANSFER
Vol. 10, No. 2, April–June 1996

Application of a Genetic Algorithm to the Optical Characterization of Propellant Smoke

Matthew R. Jones*
University of Arizona, Tucson, Arizona 85721
M. Quinn Brewster†
University of Illinois at Urbana–Champaign, Urbana, Illinois 61801
and
Yukio Yamada‡
Agency of Industrial Science and Technology, Tsukuba, Ibaraki 305, Japan

A search procedure based on a genetic algorithm is used to determine the optical properties and the particle size distribution function of propellant smoke from angular light-scattering measurements. The optical properties and size distribution parameters are obtained by matching theoretical values with measurements of the light scattered by smoke extracted from the plume of propellants that contain aluminum, magnesium, or zirconium carbide. A genetic algorithm is used to find the theoretical scattering pattern that best fits the measured scattering pattern. The measurements presented in this article were not made in situ, and so the results do not accurately reflect the optical properties and size distribution parameters of smoke found in rocket motors and plumes. However, the retrieved optical properties are in agreement with values available in the literature, and the retrieved size distributions are consistent with expectations based on analysis of the sampling method. Therefore, it is clear that the proposed inversion algorithm could be used to determine the optical properties and size distribution parameters from in situ light-scattering measurements if such measurements were available.

Nomenclature

C = angular-scattering cross sections
d = particle diameter
$dC/d\Omega$ = differential-scattering cross sections
d_{32} = mean optical size or Sauter mean diameter
f = particle size distribution function
$\tilde{f}$ = distribution of sizes and optical properties
k = absorption index
N_c = particle number concentration
n = refractive index
p = probability
r = particle radius
V = volume
$\Delta\hat{\mu}$ = uncertainty in the normalized angular-scattering coefficients
$\Delta\Omega$ = solid angle
δ = Dirac delta function
λ = wavelength
μ = angular-scattering coefficient
$\hat{\mu}$ = normalized angular-scattering coefficient
σ = geometric standard deviation
ϕ = fitness function
Ω = direction

Subscripts
c = crossover
f = final
j = index
m = mean value, mutation
max = maximum
s = solution
0 = initial

Superscripts
av = average
m = measured
t = theoretical

Received July 21, 1995; revision received Dec. 4, 1995; accepted for publication Dec. 5, 1995.

*Assistant Professor, Department of Aerospace and Mechanical Engineering, Aero Building 16.
†Professor, Department of Mechanical and Industrial Engineering, 1206 West Green Street. Associate Fellow AIAA.
‡Division Chief, Biomechanics Division, Mechanical Engineering Laboratory, Namiki 1-2.

Introduction

ADDITIVES such as aluminum, magnesium, and zirconium carbide are included in formulations of solid propellant rocket motors to increase motor performance and suppress high-frequency combustion instabilities. The combustion of these additives results in metallic oxide particles that dramatically affect the optical characteristics of the plume. Radiative emission from rocket plumes plays a significant role in the design process because of the radiant heat feedback to the nozzle, insulator surfaces, and surface of the propellant. Radiation emitted from the exhaust plumes also plays a role in the detection and identification of missiles. The particle size distribution function (PSDF) of the condensed phase particulates is one of the most important parameters needed to predict thermal radiation as well as the two-phase flow losses in a rocket nozzle. To assess the effects of smoke on motor performance and to characterize the radiation emitted from plumes, the PSDF and the optical properties of the metallic oxide smoke need to be determined.[1–6]

It has been well established that smoke produced by propellants containing aluminum is composed primarily of Al_2O_3, and that the smoke produced by propellants containing magnesium is composed primarily of MgO. Reed[7] states that based on thermochemical equilibrium calculations, ZrC should burn to ZrO_2 in a rocket motor chamber. However, the degree to which ZrC actually oxidizes to ZrO_2 is unknown.

Because of the important role played by smoke particles in the performance of a rocket motor, particle characterization techniques are of great interest.[8] Commonly used particle-sizing techniques have been reviewed by Koo[9] and Brewster.[10] Koo recommended the complementary use of mechanical or collection techniques and light extinction techniques. Collection techniques are advantageous in that they are fairly inexpensive and straightforward, but it is difficult to obtain uncontaminated samples that accurately represent the particles in the flame. Collection techniques also involve tedious data reduction and are easily biased during sample preparation. Light-scattering and absorption measurements can be made unobtrusively, and so they have a tremendous advantage over collection techniques in this regard. However, analysis of data obtained using optical techniques generally requires knowledge of the optical properties of the smoke particles. Nelson[3] reports that optical property data for smoke from solid propellant rocket motors are sparse and that the use of the available data often requires considerable extrapolation. Calia et al.[11] and Parker et al.[12] used a shock tube to heat rocket exhausted Al_2O_3 particles and measured the optical properties of the particles over a wide range of wavelengths and at elevated temperatures. However, in both of these papers the authors commented on the possible contamination of the samples during collection. These results illustrate the need to develop in situ smoke characterization techniques.

Parry and Brewster[13] reported the development of an in situ light-scattering and extinction technique for determining the optical constants and mean optical size of molten Al_2O_3 smoke particles. However, the inversion process required by this technique is tedious and computationally intensive.

The purpose of this article is to investigate the possibility of determining both the PSDF and the refractive index of propellant smoke from angular light-scattering measurements. Experiments were conducted in which smoke was extracted from the plume of a propellant strand, and measurements of the angular-scattering patterns were obtained using a multichannel polar nephelometer. A random search procedure based on a genetic algorithm was used to obtain the optical properties and parameters that characterize the PSDF of the smoke. Propellants containing aluminum, magnesium, or zirconium carbide were used in the experiments.

Light-Scattering Measurements

A 15-channel polar nephelometer was used to measure the light scattered by the smoke particles. The nephelometer's detectors are located between 23–129 deg, and are positioned such that they are equidistant in $\sin(\theta/2)$. The nephelometer's light source is an unpolarized laser beam emitted by GaAlAs laser diode with a wavelength of 0.84 μm. Figure 1 shows the primary components of the nephelometer. Smoke particles are entrained in the airstream that passes through the center of the scattering chamber and intersects the laser beam. The laser light scattered within the acceptance cone of each detector is measured by photodiodes. A complete description of the nephelometer and its calibration and operation is given by Jones.[14]

The measurements reported in this study were obtained when the inlet to the nephelometer was positioned perpendicular to the axis of the plume. Previous studies have shown that the PSDF of Al_2O_3 particles produced in propellant combustion is bimodal. The smaller mode is composed of primarily submicron smoke that is produced by detached, vapor-phase oxidation of the aluminum. The larger mode (10–100 μm) is produced by surface oxidation and condensation of the smoke on the surface of the particle.[6,8,10] Since the inlet to the nephelometer was positioned perpendicular to the axis of the plume in this experiment, the momentum of the large smoke and particles formed by droplet burnout or by coalescence carried most of them past the inlet. Therefore, the size distributions obtained in this study are biased toward the smaller smoke and are not representative of the size distributions found in rocket motors and plumes. The optical properties of the smoke particles depend on their temperature.[15] Since the smoke cools as it is drawn into the nephelometer, the optical properties obtained in this study correspond to temperatures that are significantly lower than that of the rocket chamber or the hotter regions of the plume. However, the optical constants obtained in this study could be considered representative of the smoke particles found in the cooler regions of the rocket plume.

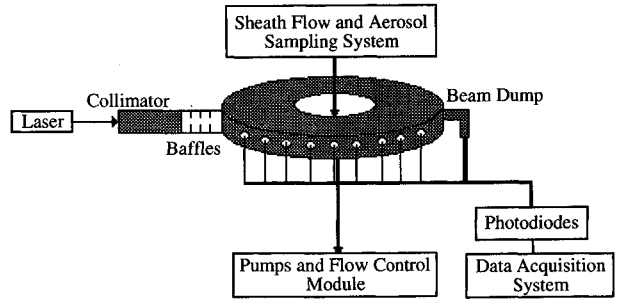

Fig. 1 Multichannel polar nephelometer.

The smoke from three different propellants was examined in this study. All of the propellants were ammonium perchlorate-based propellants and used hydroxyl-terminated polybutadiene (HTPB) as binder. The first propellant contained 10% aluminum by weight, and the second propellant contained 10% magnesium by weight. The detailed formulations of these propellants are given by Ishihara.[16] The third propellant was a reduced smoke propellant that contained 0.442% zirconium carbide.

Theoretical Model of the Light-Scattering Measurements

The nephelometer simultaneously measures the power scattered in the direction of each of its 15 detectors. The ratio of the power scattered in the direction of a particular detector to the incident irradiance is defined as an angular scattering cross section. Assuming single scattering, the angular scattering cross section measured by the jth detector C_j is related to the distribution of sizes and optical properties by the following equation:

$$C_j = \int_{V_j}\int_{\Delta\Omega_j}\int_{k_0}^{k_f}\int_{n_0}^{n_f}\int_{r_0}^{r_f} N_c \tilde{f}(r, n, k)\,\frac{dC_j}{d\Omega}(\Omega, r, n, k) \times dr\,dn\,dk\,d\Omega\,dV \quad (1)$$

The following assumptions are made to reduce the complexity of Eq. (1):

1) It is assumed that the smoke is composed of homogenous spheres. Because of high surface tension, Al_2O_3 smoke particles are highly spherical; but it is uncertain whether or not MgO and ZrO_2 smoke can be accurately modeled as spherical particles.[7] Nevertheless, predictions of plume radiation properties are generally based on the assumption that the particles are spherical, and so the determination of the effective spherical properties of this smoke is of value. Based on the assumption that the particles are spherical, the differential-scattering cross sections can be calculated from Mie theory.[17]

2) It is assumed that all of the particles have the same optical properties. Therefore, the distribution function may be written as the product of the PSDF and two Dirac delta functions:

$$\tilde{f}(r, n, k) = f(r)\delta(n - n_s)\delta(k - k_s) \quad (2)$$

3) It is assumed that the particle number density is uniform over the scattering volume.

4) It is assumed that the solid angles subtended by the detectors are small, and so the integral over Ω can be replaced

by the product of the average of the differential scattering cross sections and the solid angle subtended by each detector:

$$\int_{\Delta\Omega_j} \frac{dC_j}{d\Omega}(\Omega, r, n, k)\, d\Omega \approx \frac{dC_j^{av}}{d\Omega}(r, n, k)\Delta\Omega_j \qquad (3)$$

These assumptions simplify Eq. (1) to

$$C_j = N_c V_j \Delta\Omega_j \int_{r_i}^{r_f} f(r) \frac{dC_j^{av}}{d\Omega}(r, n_s, k_s)\, dr \qquad (4)$$

The scattering volume and the solid angle subtended by each detector depend on the geometry of the nephelometer. When comparing the measurements to theoretical values, it is convenient to remove the dependence on the geometry of the nephelometer. For this purpose, angular scattering coefficients are defined as the angular scattering cross sections divided by the scattering volume and by the solid angle subtended by each detector:

$$\mu_j = C_j / V_j \Delta\Omega_j \qquad (5)$$

It can be seen from Eqs. (5) and (6) that the unknown parameters are the particle number concentration, the PSDF, and the differential scattering cross sections. A quantity that depends only on the PSDF and the differential scattering cross sections may be obtained by normalizing the angular-scattering coefficients by their mean:

$$\hat{\mu}_j = 15\mu_j \Big/ \sum_{i=1}^{15} \mu_i \qquad (6)$$

Calculation of the theoretical angular-scattering coefficients requires that the functional form of the PSDF be assumed. Salita[8,18] reported that the PSDF of combustion-generated Al_2O_3 particles may be approximated using a bimodal log-normal distribution. Since only the smaller smoke particles were drawn into the nephelometer, the unimodal log-normal distribution given by Eq. (7) was assumed as the functional form of the PSDF:

$$f(r) = \frac{\exp\left\{-\left[\dfrac{\ell n(r) - \ell n(r_m)}{\sqrt{2}\,\ell n(\sigma)}\right]^2\right\}}{\sqrt{8\pi} r\, \ell n(\sigma)} \qquad (7)$$

In the rare case that a large particle was drawn into the nephelometer, the amount of scattered light and the shape of the scattering pattern varied greatly, so that such measurements were easily identified and discarded.

A randomized search procedure based on a genetic algorithm was used to find the values for the refractive index, the absorption index, the mean diameter, and the geometric standard deviation that produced the best agreement between the measured and theoretical scattering patterns. The search procedure is described in the following section.

Genetic Algorithm Based Search Procedure

Genetic algorithms are randomized search procedures that are based on the principle of natural selection or survival of the fittest. Genetic algorithms have recently been applied to a wide variety of optimization problems and have been found to be very robust. Goldberg[19] presents the fundamentals of genetic algorithms in detail and describes many of the problems in which genetic algorithms have been successfully applied. Genetic algorithms only require the copying and exchanging of binary strings, and so their implementation is extremely simple. The structure of a typical genetic algorithm is shown

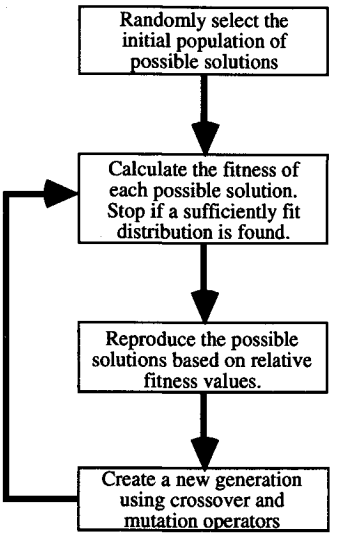

Fig. 2 Structure of a genetic algorithm.

in Fig. 2, and the following paragraphs briefly describe each of the steps illustrated in Fig. 2.

The first step in a genetic algorithm is the selection of an initial population of possible solutions. In this case possible solutions consist of values of the refractive index, the absorption index, the mean radius, and the geometric standard deviation. An initial population of 101 possible solutions was created by randomly selecting values for each of these parameters.

The second step is to define a function that will determine the fitness of each possible solution. It is customary for the fitness function to be chosen such that it assigns large values to the highly fit possible solutions and low values to the poorly fit possible solutions. Therefore, the following fitness function was used:

$$\phi(\mu^t) = \phi_{max} - \left[\sum_{j=1}^{15} (\hat{\mu}_j^m - \hat{\mu}_j^t)^2\right]^{1/2} \qquad (8)$$

The first term on the right-hand side, ϕ_{max}, was chosen to be the largest value of the objective function observed at that point in the search.

The third step is to copy possible solutions into the reproduction pool. The probability that a possible solution will be selected for reproduction is determined by its fitness relative to the other possible solutions. The reproduction operator is controlled such that there is a high probability that possible solutions with average fitness values are copied into the reproduction pool once, and that there is a low probability that any possible solution is copied into the reproduction pool more than once.

The fourth step is to create a new generation by applying the crossover and mutation operators to each of the possible solutions in the reproduction pool. Before using these operators, it is necessary to digitize each element of the possible solutions using binary strings. The crossover operator is applied by randomly selecting two digitized possible solutions from the reproduction pool. A random number is then used to determine whether or not the selected distributions are crossed. If the random number is greater than the crossover probability p_c, the selected possible solutions are copied directly into the new generation, and if the random number is less than or equal to p_c, each element of one possible solution is crossed with the corresponding element of the other possible solution. A crossover probability of 0.6 was used in this study. As with the crossover operation, whether or not the mutation operator is applied is determined by generating a random number and comparing it to the mutation probability p_m. A random number is generated for each bit in a possible solution. If the random

number is less than or equal to p_m, the value of the bit is changed. A mutation probability of 0.01 was used in this study.

After creating a new generation of digitized possible solutions, each of the possible solutions are decoded and theoretical values of the angular-scattering coefficients are calculated. The fitness values of the new distributions are calculated, and the cycle is repeated until a solution is obtained.

Results

It is possible that more than one combination of optical properties and PSDF parameters will produce scattering patterns that are similar to the measured scattering pattern. It is generally recognized that nonuniqueness is one of the primary difficulties encountered in obtaining solutions to inverse problems. Therefore, techniques for solving inverse problems often require the use of a priori information. In this study, the probability of obtaining extraneous solutions is reduced by carefully selecting the parameter space in which the search is conducted.

The ranges over which the optical constants of Al_2O_3 and MgO are allowed to vary are determined based on previously published values. Malitson[20] reported that the refractive index of Al_2O_3 at room temperature and at $\lambda = 0.85$ μm is 1.76. Plass[21] gave a value of 1.75 for the refractive index of Al_2O_3 at $\lambda = 1.0$ μm, and a value of 1.72 for the refractive index of MgO at $\lambda = 1.0$ μm. He also reported that the absorption index for both Al_2O_3 and MgO at $\lambda = 1.0$ μm is on the order of 10^{-6}. In a later study, Plass[22] indicated that the refractive index of Al_2O_3 at $\lambda = 1.0$ μm varies between 1.78 at 1200°C and 1.81 at 2020°C. To select the parameter range for the smoke produced by the propellant that contained zirconium carbide, it is assumed that the smoke is composed primarily of ZrO_2. Rujkorakarn and Sites[23] reported that the refractive index of thin ZrO_2 films varies between 2.0–2.2, and that the absorption index is on the order of 10^{-3} at $\lambda = 0.6$ μm. Based on these results, the ranges for the optical constants listed in Table 1 were selected.

Salita[8] and Parry and Brewster[13] report that the size of Al_2O_3 smoke is approximately 1 μm. However, the method used to draw the smoke into the scattering chamber of the nephelometer biased the PSDF toward the smaller smoke particles. Based on these considerations, the PSDF parameters listed in Table 1 were selected.

The measured normalized angular-scattering coefficients for smoke produced by the aluminized propellant are shown in Fig. 3. The solid curve shown in Fig. 3 is the scattering pattern that was calculated using the refractive index and size distribution parameters shown in the Al_2O_3 column of Table 2. The values of optical properties obtained in this study agree well with previously published values.

The measured normalized angular-scattering coefficients for the smoke produced by the magnesium-containing propellant

Table 1 Ranges of optical properties and size distribution parameters

	Al_2O_3	MgO	ZrO_2
n, $\lambda = 0.84$ μm	1.7–1.9	1.6–1.8	2.0–2.2
k, $\lambda = 0.84$ μm	10^{-6}–10^{-4}	10^{-6}–10^{-4}	10^{-4}–10^{-2}
Mean radius d_m, μm	0.001–1.0	0.001–1.0	0.001–1.0
σ	2.0–3.5	2.0–3.5	2.0–3.5

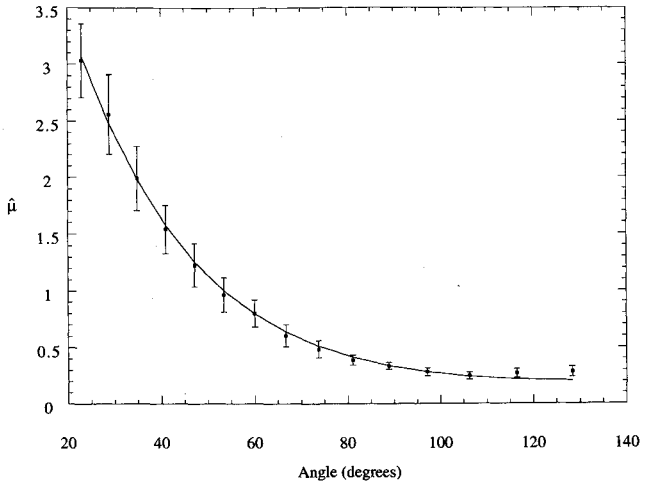

Fig. 3 Normalized angular-scattering coefficients for Al_2O_3.

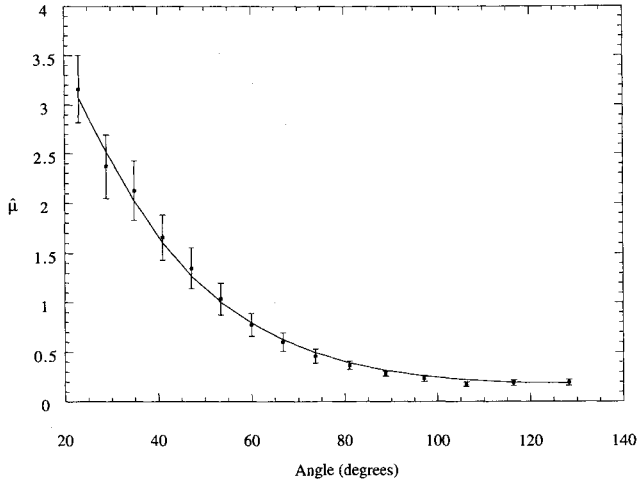

Fig. 4 Normalized angular-scattering coefficients for MgO.

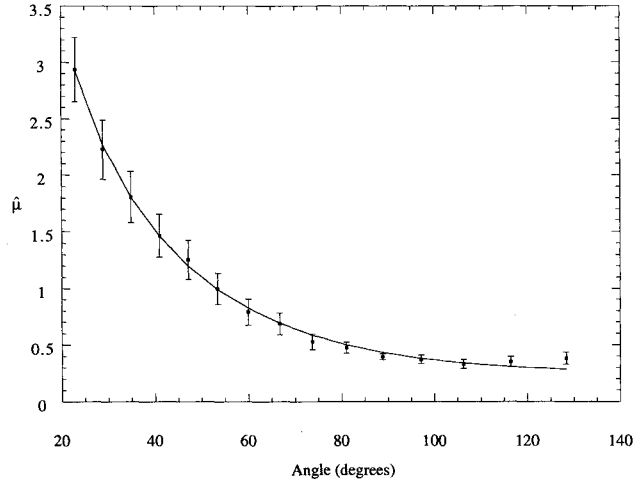

Fig. 5 Normalized angular-scattering coefficients for ZrO_2.

Table 2 Retrieved optical properties and size distribution parameters

	Al_2O_3	MgO	ZrO_2
n, $\lambda = 0.84$ μm	1.78	1.69	2.09
k, $\lambda = 0.84$ μm	4.4×10^{-6}	4.8×10^{-6}	1.0×10^{-3}
Mean diameter, d_m, μm	0.03	0.03	0.07
Mean optical size, d_{32}, μm	0.35	0.20	0.99
σ	2.7	2.4	2.8

Table 3 Normalized angular-scattering coefficients and uncertainties

	Al_2O_3		MgO		ZrO_2	
Angle, deg	$\hat{\mu}$	$\Delta\hat{\mu}$	$\hat{\mu}$	$\Delta\hat{\mu}$	$\hat{\mu}$	$\Delta\hat{\mu}$
23.1	3.03	0.33	3.16	0.34	2.94	0.29
29.0	2.56	0.35	2.37	0.32	2.23	0.26
34.9	1.99	0.28	2.13	0.30	1.81	0.23
41.0	1.54	0.21	1.66	0.22	1.47	0.19
47.2	1.23	0.19	1.35	0.21	1.26	0.17
53.5	0.96	0.15	1.04	0.16	1.00	0.14
60.0	0.80	0.12	0.78	0.12	0.79	0.12
66.7	0.60	0.10	0.60	0.09	0.69	0.10
73.7	0.48	0.08	0.46	0.07	0.53	0.07
81.1	0.39	0.05	0.37	0.04	0.48	0.05
88.9	0.33	0.03	0.28	0.02	0.39	0.03
97.2	0.28	0.04	0.24	0.03	0.37	0.04
106.3	0.25	0.03	0.18	0.02	0.33	0.04
116.4	0.27	0.04	0.19	0.03	0.35	0.05
128.3	0.28	0.04	0.20	0.03	0.38	0.05

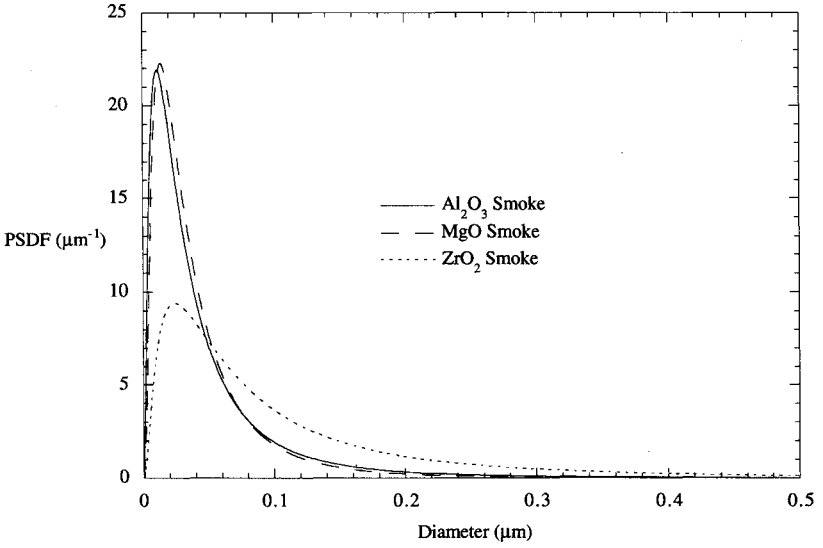

Fig. 6 PSDFs.

are shown in Fig. 4. The solid curve shown in Fig. 4 was calculated using the parameters listed in the MgO column of Table 2. The refractive index and the absorption index of MgO obtained in this study are also in relatively good agreement with previously published values.

The measured normalized angular-scattering coefficients for the smoke produced by the zirconium carbide-containing propellant are shown in Fig. 5. The solid curve shown in Fig. 5 was calculated using the parameters listed in the last column of Table 2. The values of the optical properties obtained in this study are consistent with previously published values for ZrO_2. This result supports the assumption that the smoke produced by propellants that contain zirconium carbide is composed primarily of ZrO_2.

The retrieved PSDF for each type of smoke are plotted in Fig. 6. These PSDF were used to calculate the optical mean sizes listed in Table 2. The mean optical size for Al_2O_3 smoke ($d_{32} = 0.35$ μm) obtained in this study is significantly less than the value of approximately 1.0 μm reported by Salita[8] and by Parry and Brewster.[13] However, this is to be expected since the sampling method biased the size distribution toward the smaller smoke particles. Use of the available nephelometer required that the inlet to the nephelometer be aligned perpendicular to the axis of the plume, and so it was not possible to obtain unbiased size distributions. However, the inversion procedure described in this article could be applied to measurements obtained on unbiased size distributions within the flame. To obtain measurements within the flame it would be necessary to design and construct a nephelometer that allows propellants to be burned within the scattering chamber. A system capable of adjusting the position of the propellant strand such that the distance from the burning surface to the plane defined by the laser beam and the detectors remained constant would also be necessary. Other experimental obstacles such as beam steering because of density fluctuations in the flame would also need to be addressed.

Summary and Conclusions

A technique capable of determining the optical properties and the PSDF of propellant smoke from angular light-scattering measurements has been described. Experiments were conducted in which smoke from the plume of propellants that contain aluminum, magnesium, or zirconium carbide was drawn into the scattering chamber of a multichannel polar nephelometer. A model of the scattering process was developed and the smoke particles were characterized by matching theoretical values of the angular-scattering coefficients with the 15 measured values. A random search procedure based on a genetic algorithm was used to obtain the optical properties and size distribution parameters that resulted in the best fit of the measured scattering pattern.

Note that these results were obtained using a random search procedure, and so it cannot be proved that the solutions are unique. However, the good agreement between the refractive indices of Al_2O_3 and MgO reported in this article and previously published values gives confidence that the results ob-

tained in this study are accurate. The scattering measurements and associated uncertainties are listed in Table 3 to assist those who may want to analyze the data using different inversion algorithms.

Although it was not possible to obtain measurements of the smoke particles within the propellant flame, the inversion procedure proposed in this article would have been applicable if such measurements could have been obtained. The refractive and absorption indices of the smoke particles examined in this study are representative of smoke particles found in the cooler regions of a rocket plume. Therefore, the complex refractive indices reported in this article are useful to researchers who are interested in using optical techniques to analyze plumes. These measurements begin to fill the need for an expanded database for the refractive index of metal oxide smokes. Such data are essential to perform accurate calculations of the radiative transfer in rocket plumes.

Acknowledgments

The authors thank Keng Leong of Argonne National Laboratory for allowing them to use the multichannel polar nephelometer. The authors also thank Clark Mikkelsen of the U.S. Army Missile Command for providing the propellant that contained zirconium carbide.

References

[1]Dobbins, R. A., and Strand, L. D., "A Comparison of Two Methods of Measuring Particle Size of Al_2O_3 Produced by a Small Rocket Motor," *AIAA Journal*, Vol. 8, No. 9, 1970, pp. 1544–1550.

[2]Hermsen, R. W., "Aluminum Oxide Particle Size for Solid Rocket Motor Performance Prediction," *Journal of Spacecraft and Rockets*, Vol. 18, No. 6, 1981, pp. 483–490.

[3]Nelson, H. F., "Influence of Particulates on Infrared Emission from Tactical Rocket Exhausts," *Journal of Spacecraft and Rockets*, Vol. 21, No. 5, 1984, pp. 425–432.

[4]Edwards, D. K., and Babikian, D. S., "Radiation from a Nongray Scattering Emitting and Absorbing SRM Plume," AIAA Paper 89-1721, June 1989.

[5]Traineau, J. C., Kuentzmann, P., Prévost, M., Tarrin, P., and Delfour, A., "Particle Size Distribution Measurements in a Subscale Motor for the Ariane 5 Solid Rocket Booster," AIAA Paper 92-3049, July 1992.

[6]Price, E. W., and Sigman, R. K., "The Al and Al_2O_3 Droplet Cloud in Solid Rocket Motors," *Proceedings of the 31st JANNAF Combustion Meeting*, Vol. I, Chemical Propulsion Information Agency Publication 620, Pittsburgh, PA, 1994, pp. 19–28.

[7]Reed, R. A., "Summary of Al_2O_3 Plume Characteristics and Behavior," *Proceedings of the 21st JANNAF Exhaust Plume Technology Subcommittee Meeting*, Vol. II, Chemical Propulsion Information Agency Publication 621, Pittsburgh, PA, 1994, pp. 1–10.

[8]Salita, M., "Survey of Recent Al_2O_3 Droplet Size Data in Solid Rocket Chambers, Nozzles, and Plumes," *Proceedings of the 31st JANNAF Combustion Meeting*, Vol. I, Chemical Propulsion Information Agency Publication 620, Pittsburgh, PA, 1994, pp. 1–17.

[9]Koo, J. H., "A Review of Particle Sizing Methods in Rocket Propulsion," *Proceedings of the 24th JANNAF Combustion Meeting*, Vol. 1, Chemical Propulsion Information Agency Publication 476, Pittsburgh, PA, 1987, pp. 141–156.

[10]Brewster, M. Q., "Heat Transfer in Heterogeneous Propellant Combustion Systems," *Annual Review of Heat Transfer*, edited by C. L. Tien, Vol. 4, Hemisphere, Washington, DC, 1992, pp. 287–324.

[11]Calia, V., Celentano, A., Soel, M., Konopka, W., Gutowski, R., and Ryan, R., "Measurements of UV/VIS/LWIR Optical Properties of Al_2O_3 Particles," *Proceedings of the 18th JANNAF Plume Meeting*, Chemical Propulsion Information Agency Publication 530, Pittsburgh, PA, 1989, pp. 183–192.

[12]Parker, T. E., Foutter, R. R., Person, J. C., and Rawlins, W. T., "Experimental Measurements of the Optical Properties of Al_2O_3 and Rocket Exhaust Particles at High Temperatures," *Proceedings of the 18th JANNAF Plume Meeting*, Chemical Propulsion Information Agency Publication 530, Pittsburgh, PA, 1989, pp. 193–201.

[13]Parry, D. L., and Brewster, M. Q., "Optical Constants of Al_2O_3 Smoke in Propellant Flames," *Journal of Thermophysics and Heat Transfer*, Vol. 5, No. 2, 1991, pp. 142–149.

[14]Jones, M. R., "Inversion of Light Scattering Measurements for Particle Size and Optical Constants," Ph.D. Dissertation, Univ. of Illinois, Urbana, IL, 1993.

[15]Reed, R. A., Calia, V. S., Weber, J. K. R., Krishnan, S., and McKee, M., "New Measurements and Modeling of Liquid Aluminum Oxide," *Proceedings of the 20th JANNAF Exhaust Plume Technology Subcommittee Meeting*, Vol. I, Chemical Propulsion Information Agency Publication 595, Pittsburgh, PA, 1993, pp. 467–479.

[16]Ishihara, A., "The Effect of Radiative Heat Feedback on Burning Rate of Metalized Propellants," Ph.D. Dissertation, Univ. of Illinois, Urbana, IL, 1991.

[17]Bohren, C. F., and Huffman, D. R., *Absorption and Scattering of Light by Small Particles*, Wiley, New York, 1983.

[18]Salita, M., "Quench Bomb Investigation of Al_2O_3 Formation from Solid Rocket Propellants (Part II): Analysis of Data," *Proceedings of the 25th JANNAF Combustion Meeting*, Vol. 1, Chemical Propulsion Information Agency Publication 498, Pittsburgh, PA, 1988, pp. 185–197.

[19]Goldberg, D. E., *Genetic Algorithms in Search, Optimization, and Machine Learning*, Addison–Wesley, Reading, MA, 1989.

[20]Malitson, I. H., "Refraction and Dispersion of Synthetic Sapphire," *Journal of the Optical Society of America*, Vol. 52, No. 12, 1962, pp. 1377–1379.

[21]Plass, G. N., "Mie Scattering and Absorption Cross Sections for Aluminum Oxide and Magnesium Oxide," *Applied Optics*, Vol. 3, No. 7, 1964, pp. 867–872.

[22]Plass, G. N., "Temperature Dependence of the Mie Scattering and Absorption Cross Sections for Aluminum Oxide," *Applied Optics*, Vol. 4, No. 12, 1965, pp. 1616–1619.

[23]Rujkorakarn, R., and Sites, J. R., "Crystallization of Zirconia Films by Thermal Annealing," *Journal of Vacuum Science and Technology A*, Vol. 4, No. 3, 1986, pp. 568–571.